CIAMTIS
U.S. DOT Region 3 University Transportation Center

PROJECT SUMMARY

THE CENTER FOR INTEGRATED ASSET MANAGEMENT FOR MULTI-MODAL TRANSPORTATION INFRASTRUCTURE SYSTEMS

DEVELOPMENT OF A PRACTICAL RISK FRAMEWORK FOR RAILWAY BRIDGE STIFFNESS TRANSITIONS

This document is a technical summary of the CIAMTIS report, *Development of a Practical Risk Framework for Railway Bridge Stiffness Transitions*, funded as part of the US DOT Region 3 University Transportation Center.

INTRODUCTION

Railway bridges often suffer accelerated degradation at bridge approaches due to an abrupt change in vertical track stiffness. As a train travels from ballasted track onto a bridge, the sudden change in vertical track support stiffness (from softer track to stiffer track) results in dynamic impact forces that cause a degradation of track geometry, resulting in poor ride quality and damage to track components, vehicle/lading components, and bridge components. As the geometry at this location degrades, the impact forces are exacerbated, resulting in an accelerated rate of geometry degradation and differential settlement. This results in accelerated rates of component failure as well as a significant increase in track maintenance (surfacing of the track). This cost has been estimated at well over $200M annually for U.S. railways (Stark et al., 2016).

Understanding the mechanics of this problem has been the focus of much research (Kerr, 2003). The track can be modeled as a beam on elastic foundation with the transition modeled as a step function change in stiffness. The governing equation and model are shown in Figure 1 (Zarembski et al., 1999). Numerous researchers have focused their attention on the levels of impact forces for various stiffness differentials and resulting damage.

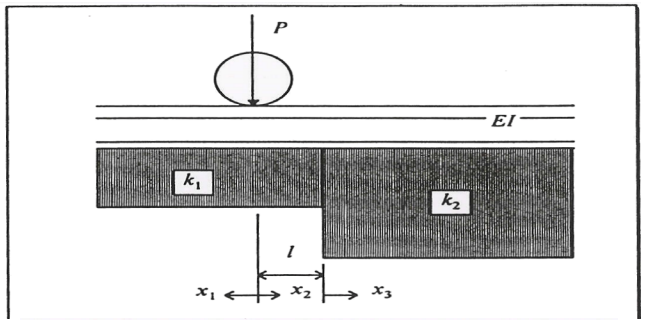

Figure 1. Stiffness transition model

There has also been much research on methods for alleviating these impact forces. There are two primary approaches in practice today: (1) introducing a transition from the soft stiffness of the parent track to the stiffer value inherent on the bridge, and (2) matching the parent track stiffness by softening the stiffness on the bridge. Method 1 utilizes transitions zones (of defined length based on stiffness differential, load and operating speed). These transition zones can be accomplished by using different tie sizes, elastomeric rail pads or ballast mats to gradually change stiffness, transition slabs made of concrete or asphalt (between the subgrade and ballast) to gradually change stiffness, and others (Li et al., 2010). Method 2 aims to match the stiffness on the bridge to that of the parent track by using elastomeric rail or ballast (under-tie) pads such that there is no stiffness transition (Kerr & Moroney, 1993). For all of the aforementioned remedial actions, it is important to know the stiffness differential as well as the load operating environments and speeds.

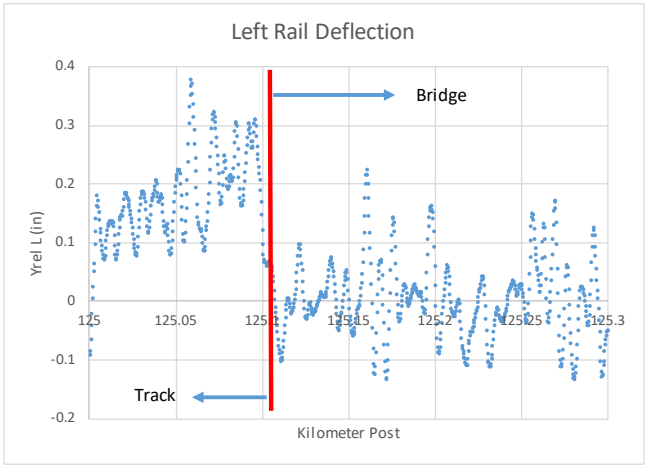

Figure 2. MRail measurement at a bridge transition

A recently introduced autonomous inspection system (MRail) measures the vertical track deflection along the track and provides the necessary data on track stiffness (Farritor, 2013) that can be used in the development of these remedial actions. In addition, as these data are collected frequently, the ability to analyze the rate of degradation of the transition area exists. Figure 2 shows

typical vertical track deflection measurements in the area of a bridge transition. Note the mean stiffness differential between zones as well as the variation around the mean, i.e. the stiffness is not uniform.

The objective of this research was to take advantage of historic measurement cycles to develop a risk index for bridge transitions that take into account the stiffness differential (mean stiffness between zones), stiffness variation (variation around the mean), train axle load, train operating speed, length of the bridge, and other factors. The data utilized to achieve this objective were vertical track deflection data and railway operating data gathered over several runs in the course of one year. These data were readily available to the research team for approximately 500 miles of railway, with nearly a hundred bridges.

METHODOLOGY

A quasi-static approach was used to determine dynamic impact force at a transition (stiffness differential, shown as ideal based on beam on elastic foundation theory in Figure 3). Two approaches were evaluated: a single sprung mass traveling and a one-eighth car freight truck model with multiple masses and spring/damper connections. The dynamic force (P_D) using a single sprung mass (m_1 with spring constant c) and slope at transition (dw/dx) is defined by the following equation, for a vehicle traveling at speed (V):

$$P_D = P_{ST} + m_1 \ddot{x}_{\max} = P_{ST} + V\sqrt{cm_1}\frac{dw}{dx}$$

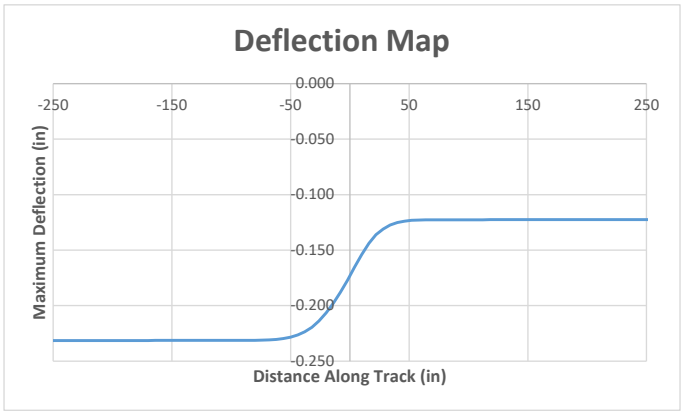

Figure 4. Deflection map for step change in stiffness

Using this type of modeling, impact factors at specified locations in track such as bridge transitions can be determined.

DATA SUMMARY

The primary focus of this study was to evaluate data that were continuously collected with respect to track stiffness. Specifically, relative track stiffness is determined using the MRail vertical track deflection measurement system, which uses a laser/camera sensor system mounted to a three-piece truck. The data that result, termed Yrel, are shown in Figure 2. Note that the data have variation along the track with two distinct means representing the transition.

A more sophisticated method for determining the dynamic impact force is to construct a single wheel dynamic simulation model that considers several masses and spring/damper connections (see Figure 4). Such a single wheel model, herein referred to as a one-eighth freight car model, or EFCM, can be constructed using Matlab/Simulink (The Mathworks, 2019). Simulink provides an intuitive object-based interface for building up a multi-degree of freedom simulation model.

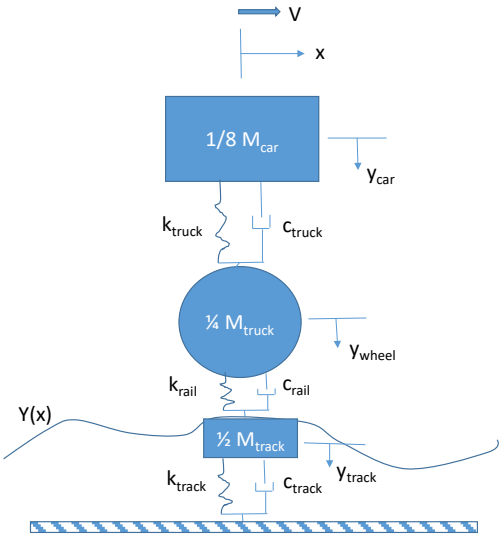

Figure 3. EFCM physical model

Data were obtained for a significant length of track on three routes (450 miles) that contained a number of bridges. These data were collected for several cycles over the course of one year. The Yrel data clearly show local deviations ("spikes") that significantly affect the dynamic forces. These forces can be greater than the force associated with the stiffness transition. Thus, filtering of the Yrel data was performed. The nonstationary multicomponent nature of the data lends itself to empirical mode decomposition (EMD) (Battista et al., 2007). This can be implemented using the Hilbert Huang Transform (HHT) (Huang et al., 1998).

As an example, the Yrel data for the left rail (from milepost 507.0 to 507.5) were analyzed using empirical mode decomposition. For this analysis, the data were transformed into the time domain, considering a 60-mph vehicle travel speed. The analysis resulted in 8 IMFs and a residual signal. By removing the high-frequency components (corresponding to IMFs 1 through 3) a smoother signal results. This is shown for comparison in Figure 5, where the black line is the original Yrel and the bolder red line is the smoothed Yrel. This type of smoothing allows for better identification of longer length stiffness variations.

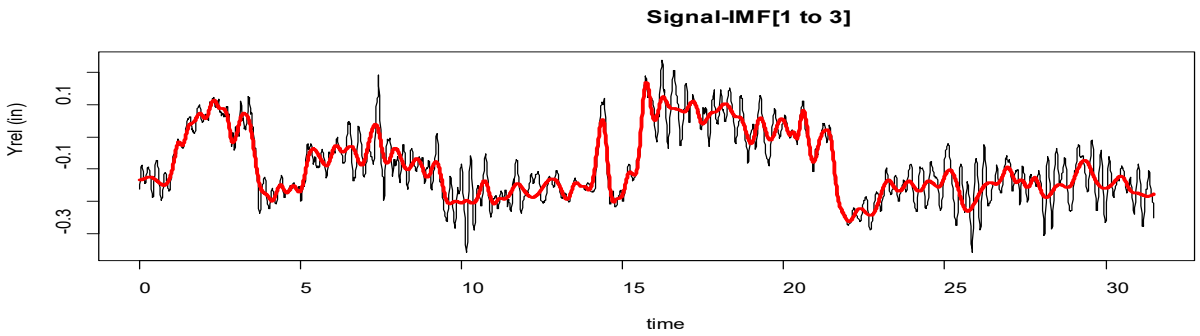

Figure 5. Original and smoothed Yrel

It is important to note that transformation into the time domain allows for a time-based forced input to be used with the simulation modeling. The actual Yrel data can in turn be used as a forced input to the dynamic simulation model. Recall that the model requires a vertical velocity input (V_y). This can be achieved by differentiating the Yrel data with respect to time for a defined vehicle speed (V), using central difference numerical differentiation, as follows:

$$V_y(t_i) \cong \frac{Yrel_{i+1} - Yrel_{i-1}}{2dt}, \quad (i = 2. \ldots ., N-1), \text{ Where } dt = \frac{dx}{V}, where\ dx = 1\ foot\ for\ this\ data$$

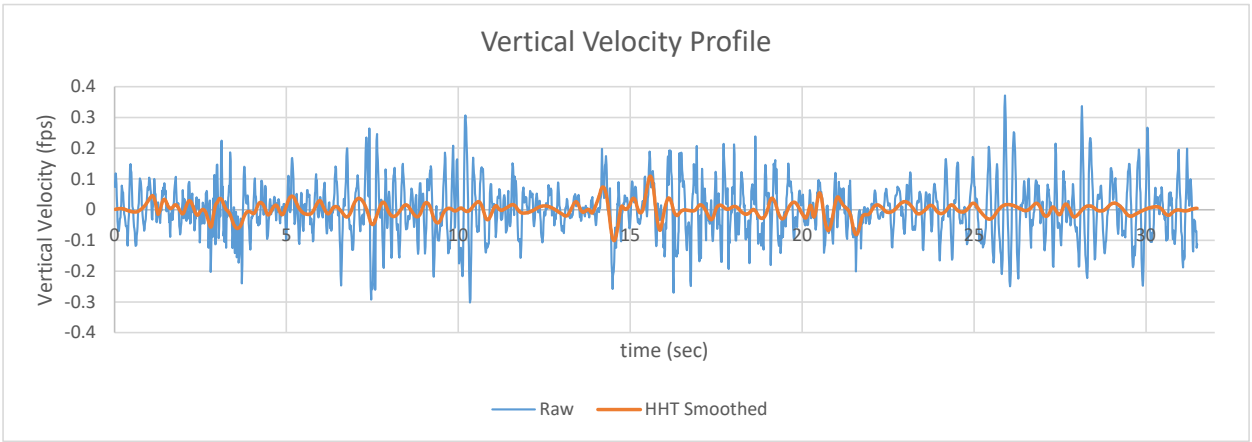

Figure 6. Vertical velocity profile

Utilizing the equation above, the resulting vertical velocity profile (vehicle traveling at 60 mph) for the left rail for a half mile of track (MP 507.0 to 507.5) based on the measured Yrel data is shown in Figure 6. The vertical velocity is shown in the time domain for the raw data and for the data smoothed using the HHT (first 3 IMFs removed) filtering technique.

EVALUATION OF RESULTS

Considering all of the above, a risk index can be created for each measurement of *Yrel*. The risk index is in the form of a dynamic load impact factor (shown at right). From this equation, the dynamic force augment can be determined from simulation modeling or some other more sophisticated simulation model. This is often impractical for large amounts of data. Alternatively, the slope method can be implemented both practically and easily, as defined in the equation. A comparison for an ECFM and the slope method is shown in Figure 7. When considering actual data, it appears that for the example shown, the slope method slightly understates the forces predicted by the Simulink model. This is particularly true in the localized location of rapid change of Yrel.

$$RISK_i = TZ_i * (1 + Pd_i/Pst)$$

Where

$$TZ_i = \begin{cases} 1, & for\ a\ defined\ transition\ zone \\ 0, & for\ everywhere\ else \end{cases}$$

$$Pd_i = \begin{cases} Pd\ from\ Simulink \\ or \\ \dfrac{(Yrel_{i+1} - Yrel_{i-1})}{x_{i+1} - x_{i-1}} V\sqrt{km} \end{cases}$$

Pst = Static wheel load

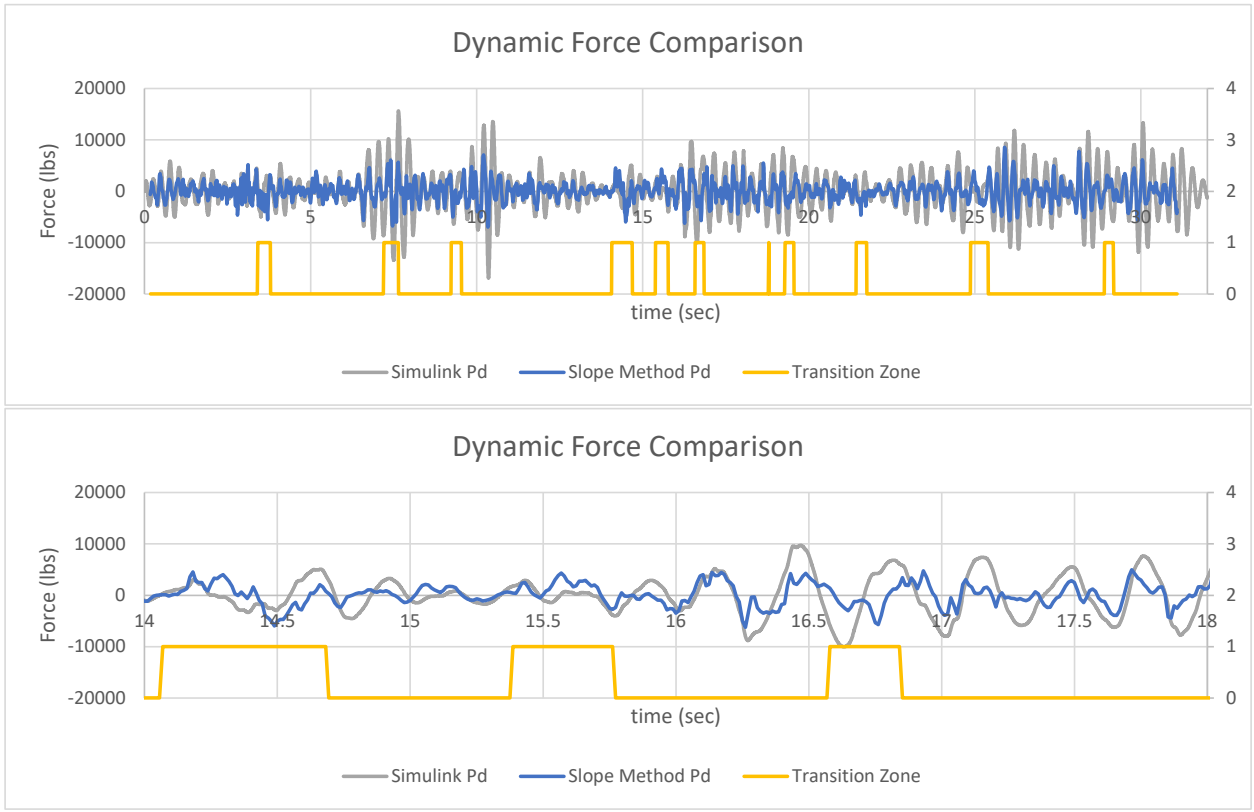

Figure 7. Transition zone comparison of Simulink and slope method

An application of the transition zone risk model presented in the previous section was performed for the three study segments utilizing the slope method equation. This approach was used based on its ease of implementation and ability to be incorporated in real time on the inspection vehicle.

Figure 8 shows an example of the application of the risk framework for MP 507.0 to 507.5. The top plot shows the left rail *Yrel* values (in units of feet) as well as the identified transition zones. The bottom plot shows the calculated risk values (impact factor) within the transition zone, along with the maximum/peak value within the zone[1]. Note that the risk value within the zone traverses around 1.0. This is due to the dynamic force interaction within the zone, and the maximum, or peak, value is of interest.

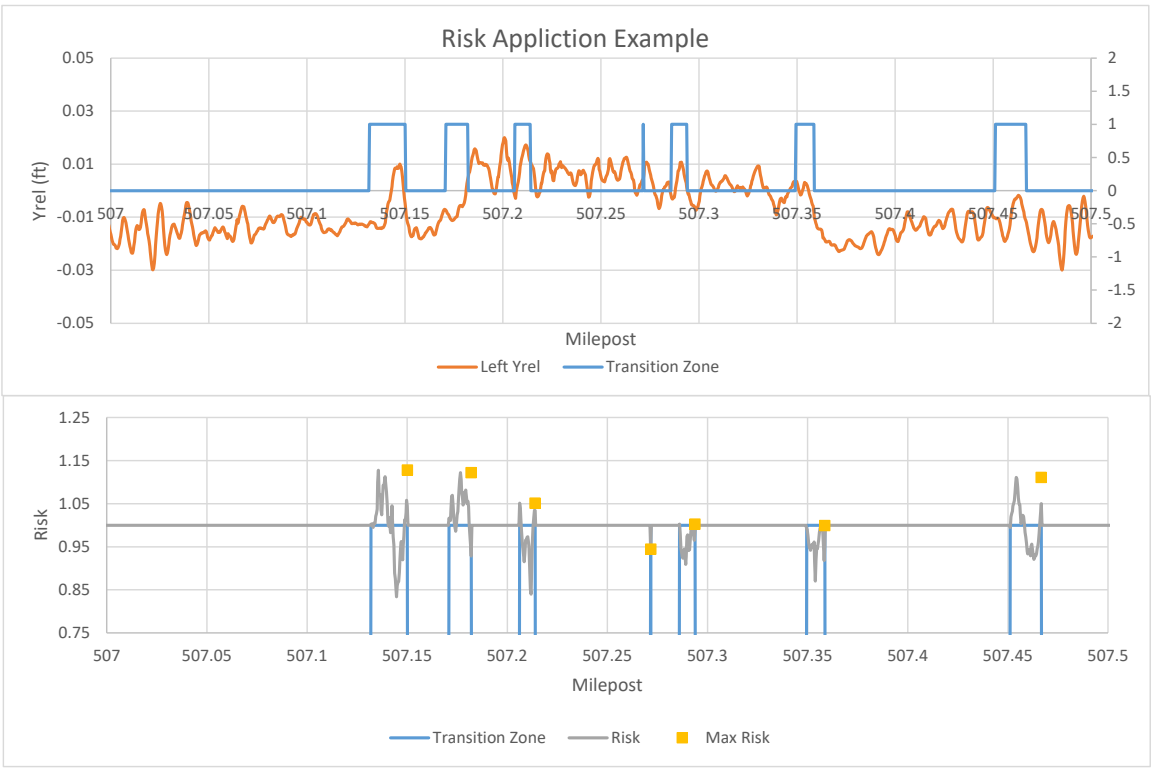

Figure 8. Example application of risk framework

This same approach was applied for the entire length of track in each of the three study segments. Thus, for more than 100 miles of track, the transition zones were identified and the maximum risk factor calculated for each transition zone.

In order to understand the distribution of resulting risk values, Figure 9 shows the probability density function and cumulative density function for each rail, for one of the study segments. This figure shows the mean and variation of the risk factors, allowing for classification of a transition with respect to risk associated with dynamic impact. The average risk in the transition zone area ranges from 1.11 to 1.16.

Given the distribution, it is reasonable to set thresholds for classifying the transitions. The average range of risk was shown to be 1.11 to 1.16 (which is a dynamic impact factor), which is consistent with report values of > 1.1 from previous studies (Plotkin et al., 2006). Thus, for exemplary purposes, the following thresholds[2] were set, as shown in Table 1.

Table 2 allows for quickly identifying the number of transition zones that fall into a given category. Note that segment AB has a much larger proportion of segments in the poorer categories (higher risk factor). This is most likely due to the measurement equipment issues reported. In addition, the data allow for determining the total length of transitions in various maintenance categories for defining maintenance requirements.

[1] The maximum value is the yellow square shown at the end of the zone and is considering the maximum risk value for the entire zone.

[2] Note: these thresholds are representative and further research is required to establish appropriate thresholds.

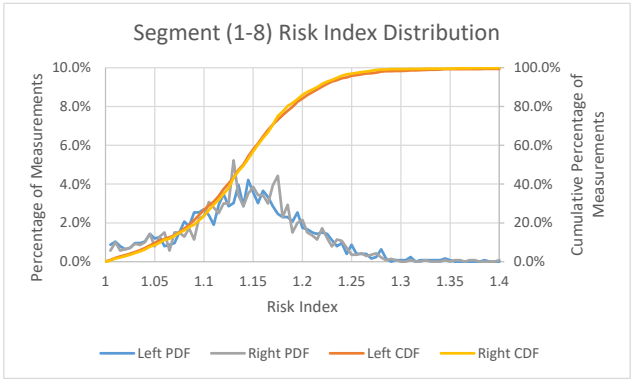

Figure 9. Max risk distibution for each study segment

Table 1. Example risk thresholds

Range	Classification	Description
< 1.1	Low Risk	No action required. Behaving reasonably.
1.1–1.25	Moderate Risk	Potential for moderately accelerated degradation. Monitor.
1.25-1.4	High Risk	High risk if accelerated degradation. Candidate for further analysis.
> 1.4	Very High Risk	Candidate for remedial action such as subgrade remediation, addition of transition material, matched pads technique, etc.

Note that the above thresholds represent varying classes of maintenance and remediation requirements and do not correlate to safety, due to the low level of dynamic loading. Applying these thresholds to the risk values calculated for the three study segments results in Table 2.

Table 2. Application of thresholds summary

	Segment AB					Segment BC					Segment (1-8)			
	Left Rail		Right Rail			Left Rail		Right Rail			Left Rail		Right Rail	
	Num	Pct	Num	Pct		Num	Pct	Num	Pct		Num	Pct	Num	Pct
< 1.1	43	10.2%	218	17.6%		26	25.0%	24	30.8%		336	26.7%	330	23.6%
1.1 - 1.25	141	33.6%	748	60.5%		69	66.3%	52	66.7%		876	69.6%	1031	73.7%
1.25 - 1.4	128	30.5%	204	16.5%		6	5.8%	2	2.6%		40	3.2%	36	2.6%
> 1.4	108	25.7%	67	5.4%		3	2.9%	0	0.0%		7	0.6%	1	0.1%
	420		1237			104		78			1259		1398	

CONCLUSION AND IMPLEMENTATION

The research conducted herein was aimed at utilizing readily available track measurement data, specifically vertical track deflection data (MRail), to develop a risk index for stiffness transitions. A dynamic simulation approach was utilized to develop the risk index. It was shown that dynamic simulation modeling is an effective means for developing a dynamic impact factor at stiffness transitions, due to the abrupt change in vertical elevation as a vehicle runs over the transition zone. While commercially available, sophisticated simulation models provide multiple degrees of freedom to develop force and motions of multiple car components, the force at the track is of predominant interest. These models are complicated to implement and are computationally intensive. For the purposes of this study a simplified dynamic simulation approach was used.

Two approaches were studied: an eighth car freight model developed in MATLAB/Simulink that responds to a vertical velocity forced input, and a simplified single sprung mass with a vertical velocity impulse based on the slope of travel of the mass. The vertical velocity forced input can be developed directly from the MRail vertical track deflection measurement data and the vehicle speed. This vertical velocity input can be input to the dynamic simulation model (either method described above) and the dynamic force and corresponding dynamic impact factor calculated, which defines the risk index.

The results of the application to several hundred miles of inspection data showed that quite a number of stiffness transitions were identified, considerably more than the estimated number of bridges. This is to be expected as grade crossings, culverts, and other track structures will result in vertical track deflection data (MRail) that exhibit transition

zone response. In addition, naturally occurring transition zones due to significant change in subgrade characteristics will result. These transition zones varied in overall length.

The risk index was calculated for each of these zones, both the change in force throughout the zone as well as the maximum value within the zone. In order to understand the relative distribution of the resulting index values, probability density plots were developed. Based on these plots, as well as results of other researchers, a series of potential thresholds for the risk index were introduced and the transition zones classified based on these thresholds. This type of analysis allows the railroad to classify its track and develop maintenance and remediation plans for transition zones.

Implementation of this risk model, in the manner conducted herein, can be done in real time on the inspection car due to its practical nature and straightforward calculation technique, or alternatively offline using an eighth freight car model, as developed herein.

References

Battista, B. M., Knapp, C. C., Mcgee, T., & Goebel, V. (2007). Application of the Empirical Mode Decomposition and Hilbert-Huang Transform to Seismic Reflection Data, *Geophysics*, *72*(2).

Farritor, S. and Fateh, M. (2013). *Measurement of Vertical Track Deflection from a Moving Rail Car*. Federal Railroad Administration, Report No. DOT/FRA/ORD-13/08, Washington, D.C.

Huang, N. E., Shen, Z., Long, S. R., Wu, M. C., Shih, H. H., Zheng, Q., Yen, N.-C., Tung, C. C., & Liu, H. H. (1998). The empirical mode decomposition and the Hilbert spectrum for nonlinear and non-stationary time series analysis. *Proceedings of the Royal Society of London*, *454*, 903–995.

Kerr, A. D., & Moroney, B. E. (1993). Track transition problems and remedies. *AREA Bulletin 742*, *94*, American Railway Engineering Association, Washington, D.C., 267–298.

Kerr, A. D. (2003). *Fundamentals of Railway Track Engineering*. Omaha, NE: Simmonas-Boardman Books, Inc.

Li, D., Otter, D., & Carr, G. (2010). Railway bridge approaches under heavy axle load traffic: Problems, causes, and remedies. *Proceedings of the Institution of Mechanical Engineers, Part F: Journal of Rail and Rapid Transit*, *224*, 383–390.

Plotkin, D., Davis, D. D., Gurule, S., & Chrismer, S. M. (2006). Track Transitions and the Effects of Track Stiffness. In *AREMA Annual Conference*, Louisville, KY, 1–36.

Stark, T., Wilk, S., & Rose, J. (2016). Design and Performance of Well-Performing Railway Transitions. *Transportation Research Record: Journal of the Transportation Research Board*, *2545*, 20–26.

The Mathworks, I. (2019). *MATLAB.* (R2019b ed.). Natick, Massachusetts.

Zarembski, A. M., Palese, J. W., & Katz, L. (1999). Implementation of a Dynamic Rail-Highway Grade Crossing Transition. In *Transportation Research Board Annual Meeting*. Washington, D.C.

For More Information	354B DuPont Hall
Principal Investigator: Joseph W. Palese, PhD, MBA, PE	Newark, DE 19716 Phone: 302.831.3517
Technical reports when published are available at **https://r3utc.psu.edu/**	E-mail: palesezt@udel.edu